

Measurement of stress using synchrotron x-rays

Donald J Weidner¹ and Li Li

Mineral Physics Institute, Department of Geosciences, Stony Brook University, Stony Brook, NY 11794-2100, USA

E-mail: dweidner@sunysb.edu and lilli@ic.sunysb.edu

Received 6 March 2006, in final form 1 May 2006

Published 8 June 2006

Online at stacks.iop.org/JPhysCM/18/S1061

Abstract

Stress analysis in polycrystalline materials reveals that stress can vary considerably among different subpopulations of grains. Samples of MgO and mixtures of MgO and spinel have been studied. After the onset of plastic flow, stronger grains or orientations will support more stress than the weaker grains. A grain to grain fabric develops that enables this stress partitioning. The stress partitioning and the resulting fabric can invalidate static measurements of elastic moduli. However, high temperature flow mechanisms reveal a more isotropic strength behaviour resulting in a more uniform variation of stress with orientation.

(Some figures in this article are in colour only in the electronic version)

1. Introduction

For over a decade synchrotron based tools have continued to provide insights into properties of polycrystalline samples through measurement of stress inside samples at both high pressure and high temperature. The manner in which polycrystals support deviatoric stress and the implications for elastic and plastic properties have been central in these investigations.

Elastic strain anisotropy has been used to predict elastic modulus anisotropy in many diamond anvil studies using x-rays that enter the sample chamber through the gasket (Kavner 2003, Kavner and Duffy 2001, Duffy *et al* 1999b, Mao *et al* 1998, Merkel *et al* 2002). Weidner *et al* (2004) concluded that plastic anisotropy will often overprint elastic anisotropy in the strain anisotropy once plastic deformation is initiated in the sample. Thus, the deduction of single crystal elastic moduli from radial diffraction data often yields incorrect values if the sample has plastically deformed. The standard Reuss–Voigt bounds of stress which are assumed in this analysis are no longer relevant as the Taylor–Sachs bounds must prevail. Reuss–Voigt bounds assume that all of the strain is elastic, while the Taylor–Sachs bounds model strain entirely as plastic deformation resulting from dislocation systems. Thus for a given stress field, strain

¹ Author to whom any correspondence should be addressed.

anisotropy is defined by elastic anisotropy in the elastic regime (Reuss–Voigt) and by strength anisotropy in the plastic regime (Taylor–Sacks).

The question becomes: are there some instances where these measurements are valid, and are there any strategies that can overcome this problem. To the first question, we can expect that deformation processes that are isotropic may not overprint the strain field of a deforming sample. Diffusion or dynamic recrystallization are likely to drive the stress distribution to the Reuss state. A possible strategy for overcoming the effects of plastic flow on the strain anisotropy would be to anneal the sample after compression to the desired pressure. Then strain anisotropy is determined as the sample is further loaded, but in the elastic regime.

In this paper we will explore both of these possibilities. We conclude that high temperature flow may qualify to produce a Reuss stress field. However, no clear guidance is found to determine this condition *a priori*. Second, the proposed strategy of annealing before measuring the stress–strain relation requires that no fabric develops during the initial loading process. Fabrics that support large stress differences between grains in the plastic regime may also support such stress heterogeneities in the elastic regime after the stresses are relaxed. Thus, this strategy does not guarantee a successful measurement of the elastic moduli.

2. Experimental constraints

The stress measurements reported here are from the distortion of the Debye rings. The method of defining stress from a single diffraction ring has been discussed many times before (Singh *et al* 1998, Li *et al* 2004a, Duffy *et al* 1999a). Essentially the magnitude of the differential elastic strain in the plane perpendicular to the x-ray beam is derived from the departure of the Debye ring from a circle. The orientation of the stress field is defined by the orientation of the distortion. In the event that elastic moduli are not known, constraints on the elastic moduli, namely the elastic anisotropy, are inferred from the anisotropy of elastic strain. The variation of ellipticity with the crystallographic orientation responsible for the particular Debye ring is used to define strain anisotropy. The elastic moduli are related to these quantities if the stress field on all grains is uniform (the Reuss state). In this paper, we will use materials in pressure/temperature regimes where the elastic moduli are known. Thus, the strain directly defines stress for the particular population of grains that define the Debye ring. Strain anisotropy will yield the variation of stress with these different populations of grains.

Li *et al* (2004b) reported measurements of stress in an MgO sample at 500 °C. Figure 1 illustrates the measured stress using the [111] and [200] diffraction lines with several diffraction patterns as the sample is maintained at constant stress by a deformation DIA (DDIA) pressure system. One sample that was stressed at about 2/3 of the yield point exhibited a stress state intermediate between the Reuss and Voigt states, but closer to the Reuss. That is, all diffraction lines yield nearly the same stress. The sample that was stressed into yield was outside the Reuss–Voigt range and experienced a 50% greater stress measured by the [111] diffraction lines than from the [200] diffraction lines. The difference in stresses between [111] and [200] is explained by plastic flow of MgO, for which the active slip systems required different critical resolved shear stress and these systems are differently accessible to the different orientations of grains. Thus, different populations of grains, that depend on the orientation in the polycrystals, support quite different levels of stress. The observations were quantitatively simulated with a self-consistent flow model demonstrating the crucial role of plastic anisotropy for defining stress variations among subpopulations of grains.

The strain anisotropy in the case of plastically deforming MgO reflects the plastic strength anisotropy of MgO rather than the elastic moduli. The plastic strength parallel to [111] can be over an order of magnitude larger than the strength parallel to [100] (Paterson and Weaver

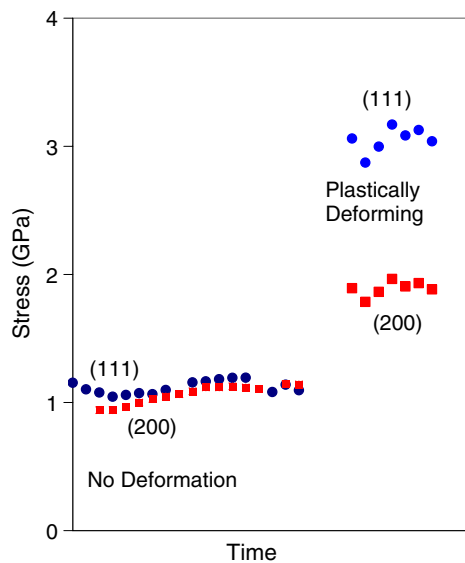


Figure 1. Differential stress in MgO samples at 500 °C during uniaxial loading in DDIA. The stress measured by two different diffraction peaks is illustrated by different symbols. The higher stressed sample plastically deformed, while the low stress sample did not. The different points represent different diffraction spectra collected during the stress cycle.

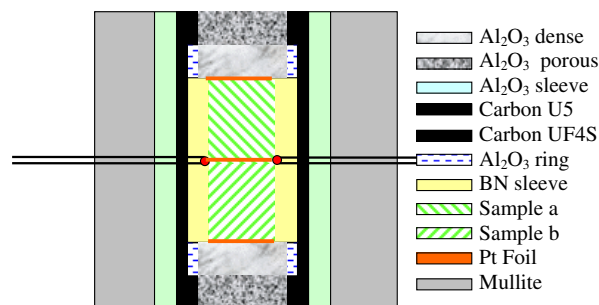


Figure 2. Illustration of sample cell for two samples (a and b).

1970). The stress was evaluated with knowledge of the elastic moduli. If, on the other hand, the elastic moduli were not known, then the data might be incorrectly interpreted to yield the elastic moduli, but with the assumption that the stress was the same for all grains.

A two-phase aggregate with different strength components can be used as a model for a material with a strong strength anisotropy. The advantage of the two-phase aggregate is that one can map out the spatial distribution of the two components to identify fabric development as a result of deformation. Furthermore, the effects of dilution can be studied.

Here we report some experimental results for a mixture of spinel (MgAl_2O_4) and MgO. In particular, we focus on data obtained during plastic flow of composites with volume distributions of 100% MgO (mgo100), 75% MgO/25% spinel (mgo75sp25), 25% MgO/75% spinel (mgo25sp75) and 100% spinel (sp100). Commercial powders of the two materials (350 mesh grain size) were mechanically mixed, cold pressed and loaded into the high pressure cell. The composites were studied in two experimental deformation runs, the first two samples in one run and the second two samples in the other run. As illustrated in figure 2, two cylindrical

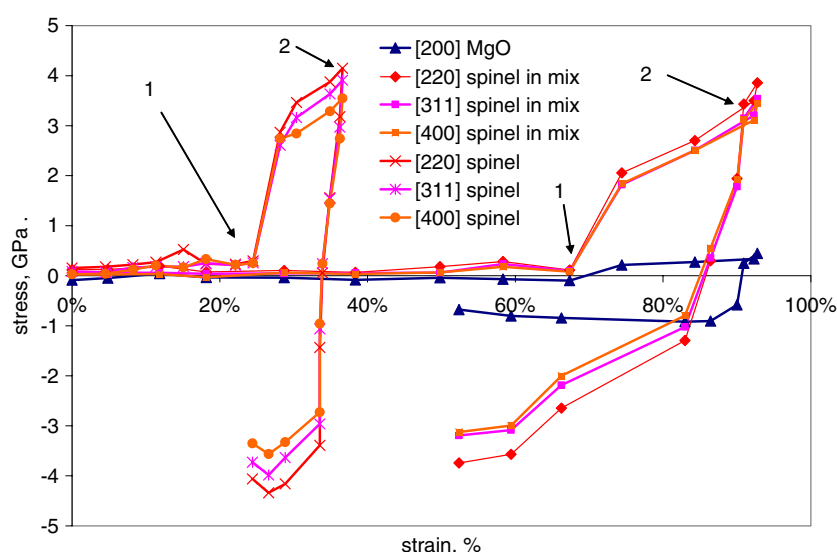


Figure 3. Stress as a function of plastic strain for two samples in the same cell. The set of curves to the right are for the 75% spinel sample which showed approximately twice the deformation of the pure spinel sample. The arrow labelled 1 indicates the lowering of the temperature from 1000 to 800 °C and the arrow labelled 2 indicates the reversal of the loading force.

samples are stacked along the unique stress axis with metal foils separating the samples and also between the sample and the corundum end piston.

Deformation experiments were performed at Brookhaven National Laboratory, beamline X17B2 in the DDIA apparatus (Durham *et al* 2002, Wang *et al* 2003). Differential stress is measured from the energy dispersive diffraction patterns recorded at 0 and 90° relative to the uniaxial compression direction (Li *et al* 2004a). Plastic strain as a function of time is defined from sample images (Li *et al* 2003, Vaughan *et al* 2000). Samples were initially compressed to 5 GPa, then annealed at 1000 °C for tens of minutes, then deformed at a strain rate of 10^{-5} s^{-1} for tens of per cent strain, temperature was then lowered to 800 °C where deformation continued. Finally, the direction of the deformation was reversed, the sample being lengthened along the unique stress axis. Figures 3 and 4 illustrate the stress versus strain for the samples. The arrow labelled as 1 indicates the point where the temperature was lowered to 800 °C and the arrow labelled as 2 indicates the reversal of the piston loading direction. Stresses at 1000 °C are near the uncertainty level of the measurement. Here we focus on the 800 °C data as they are robust and well resolved. Figure 5 summarizes the average loading stress for each material. The error bars indicate the spread of stress measurement based on different diffraction peaks. For spinel the [400], [311] and [110] diffraction lines are used, while only the [200] could be used for MgO due to the overlap of other lines with some of the spinel lines. As seen in figure 5, the stress supported by spinel is nearly the same for the 100% spinel and the 75% spinel sample but much less for the 25% spinel sample. The stress in the MgO portion of the sample is nearly the same in all mixtures. Figure 3 illustrates that the 100% spinel and the 75% spinel, which were run in the same experiment, suffered a factor of two difference in strain even though the stress in the spinel was nearly the same. Thus, the addition of 25% MgO enabled considerably more deformation.

This combination of elastic stresses and strains can guide us to an improved understanding of the range of stress–strain properties that are likely. The large difference in stress between

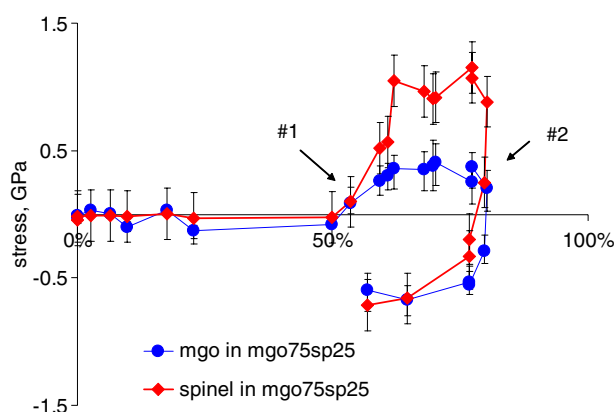


Figure 4. Stress as a function of plastic strain for the 25% spinel sample. The arrow labelled 1 indicates the lowering of the temperature from 1000 to 800 °C and the arrow labelled 2 indicates the reversal of the loading force.

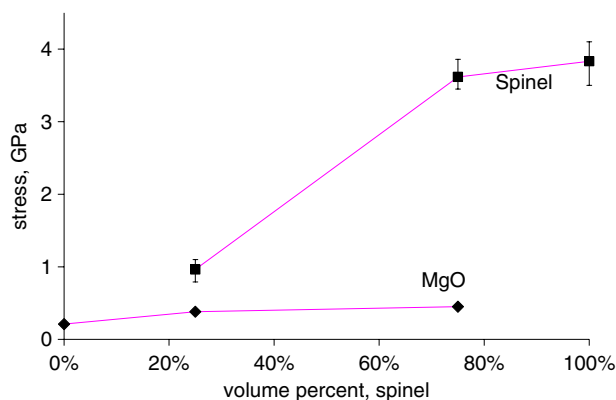


Figure 5. Average stress during loading at 800 °C for the two grain populations in a two-phase mixture as a function of volume per cent of the spinel phase. The error bars indicate the range of stresses determined from the spinel diffraction peaks, [400], [311] and [220]. Only the MgO [200] peak could be used.

the spinel grains and the MgO grains serves to illustrate that strong and weak grains can self-organize to allow the strong grains to support more stress. Even in the case of 25% spinel, we find that the stress in the spinel is about twice that of the MgO on the loading cycle. For the 75% spinel, the stress in the spinel is essentially the same as in the 100% spinel, and thus equal to the strength of the spinel sample. Still, the small amount of MgO present in this sample is responsible for the doubling of the plastic strain. In the 75% spinel sample, the MgO stress reversed sign during the extension portion of the experiment while the spinel was still under compression. This illustrates that there would remain a significant residual stress in the sample if the loading force were simply removed at this time. However, on further extension, the spinel stress continued to grow to a similar magnitude, but reversed its sign as on loading. In the sample with only 25% spinel, the stress in the spinel did not grow to its compressive magnitude during the extension phase of the experiment. Rather it attained only the stress value of the MgO portion of the sample. This indicates that upon loading, a fabric developed that enabled the strong phase to interact and support more of the stress. On the reversal of stress

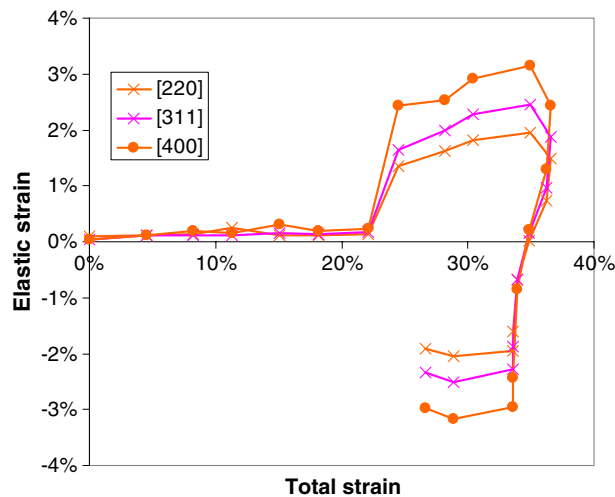


Figure 6. Elastic strain as a function of total strain in the pure spinel sample as measured for the diffraction lines [400], [311] and [220]. The range of strain between peaks is larger than for the stress, and the order is reversed.

sign, this fabric did not allow the spinel to continue to support other spinel grains, and the stress in all grains was limited by the strength of the MgO network. Thus, significant fabric develops during the long loading cycle.

These observations suggest that fabric and residual stresses can develop during a plastic deformation cycle of an experiment. These two phenomena have the potential to complicate an elastic strain anisotropy measurement of a sample that is plastically compressed and annealed. Significant errors can occur for any inference of elastic properties from such measurements unless these factors can be properly defined and modelled.

A further interesting feature in the spinel data concerns the variation in stress with diffraction peak. While figure 3 identifies the stress for each of the spinel diffraction peaks, figure 6 illustrates the elastic strain for the 100% spinel sample. The largest elastic strain is associated with the smallest stress, and vice versa. The stresses are closer to being uniform than are the strains. This combination defines the stress–strain relation between the Reuss and Voigt bounds, but closer to the Reuss bounds. Furthermore, the 5–10 μm grains were found to be relatively dislocation free in TEM observations. This distinction from the MgO sample of figure 1 indicates a more isotropic deformation process than for the MgO case. Dislocation processes can be relatively isotropic if enough dislocations systems are active. Diffusion creep will be more isotropic than dislocation glide. However, the strain rates that were measured were much too high compared with the extrapolated values from diffusion flow law of Addad *et al* (2002). We speculate that dynamic recrystallization was an important factor in the evolution of the sample. The grains remain very equant despite the large strain of the whole sample.

3. Conclusion

Derivation of elastic modulus properties from elastic strain anisotropy remains elusive. Stress partitioning among different grain populations violates the basic assumption. Plastic deformation not only deposits the stress on the strong grains, but also develops a fabric where the strong grains interact elastically. This fabric and residual stresses further complicate any

process to render a plastically deformed sample into a state where elastic measurements can be made. Nonetheless, there is a suggestion that high temperature deformation processes that involve diffusion, recrystallization and even power law creep are more isotropic than dislocation glide enabling the elastic strain anisotropy to be dominated by the elastic modulus anisotropy. This gives hope that high temperature measurements of elastic properties may be more feasible than room temperature measurements and that the uncertainty in stress that is introduced by the stress partitioning may become less in these high temperature determinations.

Acknowledgments

The authors thank the SAM group for providing technical support and Liping Wang and Zhong Zhong for their support at the at NSLS beam line. This research was carried out in part at the NSLS, which is supported by the US Department of Energy, Division of Material Sciences and Division of Chemical Sciences under contract no. DE-AC02_98CH10886 and COMPRES for support of the beam lines X17 (EAR0135554). This research was supported by the NSF grant EAR-9909266, EAR0135551, and EAR0229260. MPI publication no. 364.

References

- Addad A, Crampon J and Duclos R 2002 *J. Eur. Ceram. Soc.* **22** 329–35
- Duffy T S, Shen G Y, Heinz D L, Shu J F, Ma Y Z, Mao H K, Hemley R J and Singh A K 1999a *Phys. Rev. B* **60** 15063–73
- Duffy T S, Shen G Y, Shu J F, Mao H K, Hemley R J and Singh A K 1999b *J. Appl. Phys.* **86** 6729–36
- Durham W, Weidner D, Karato S and Wang Y 2002 *Plastic Deformation of Minerals and Rocks* vol 51, ed S Karato and R Wenk (Washington, DC: Mineralogical Society of America) pp 291–329
- Kavner A 2003 *Earth Planet. Sci. Lett.* **214** 645–54
- Kavner A and Duffy T S 2001 *Geophys. Res. Lett.* **28** 2691–4
- Li L, Raterron P, Weidner D J and Chen J 2003 *Phys. Earth Planet. Inter.* **138** 113–29
- Li L, Weidner D, Raterron P, Chen J and Vaughan M 2004a *Phys. Earth Planet. Inter.* **143** 357–67
- Li L, Weidner D J, Chen J, Vaughan M T, Davis M and Durham W B 2004b *J. Appl. Phys.* **95** 8357–65
- Mao H-k, Shu J, Shen G, Hemley R J, Li B and Singh A K 1998 *Nature* **296** 741–3
- Merkel S, Wenk H R, Shu J, Shen G, Gillet P, Mao H-k and Hemley R J 2002 *J. Geophys. Res.* **107** 2271
- Paterson M S and Weaver C W 1970 *J. Am. Ceram. Soc.* **53** 463–72
- Singh A K, Balasingh C, Mao H-k, Hemley R and Shu J 1998 *J. Appl. Phys.* **83** 7567–75
- Vaughan M, Chen J, Li L, Weidner D and Li B 2000 *AIRAPT-17* ed M H Manghnani, W J Nellis and M F Nicol (Hyderabad: Universities Press) pp 1097–8
- Wang Y B, Durham W B, Getting I C and Weidner D J 2003 *Rev. Sci. Instrum.* **74** 3002–11
- Weidner D J, Li L, Davis M and Chen J 2004 *Geophys. Res. Lett.* **31** 19090–4